Institute for Sustainable Energy, UNIVERSITY OF MALTA

SUSTAINABLE ENERGY 2015:
THE ISE ANNUAL CONFERENCE
Tuesday 17th March 2015, Dolmen Resort Hotel, Qawra, Malta

ISBN No. 978-99957-853-0-7

A PRELIMINARY COMPUTATIONAL STUDY OF FLAT ROOF CONVECTIVE THERMAL RESISTANCE IN THE PRESENCE OF PHOTOVOLTAIC PANELS

D. Micallef[1], V. Buhagiar[1] and S.P. Borg[1]

[1] Department of Environmental Design, Faculty for the Built Environment,
University of Malta, Msida, MSD 2080, Malta
Tel: (+356) 2340 2870

Corresponding Author E-mail: daniel.micallef@um.edu.mt

ABSTRACT: The effect of roof mounted photovoltaics on the heat transfer performance of roofs has primarily been investigated in the context of the resulting shading effect. The convective heat transfer coefficient will change as a result of the blockage caused by the photovoltaic panels. In this work, a quantification is given of the differences between heat transfer coefficients on a bare roof and a roof with photovoltaic panels having a specified configuration. A computational fluid dynamics approach is used. The study is only preliminary and hence a standard k-ε turbulence model is used. The presence of photovoltaics is found to increase the convective heat transfer coefficients by around 26% for a north wind. The influence on the U-Value depends on the type of roof construction but for summer conditions an increase in U-value is observed which has positive cooling effects.

Keywords: Roof CHTCs, Photovoltaics, Roof U-values, Convection on flat roofs

1 INTRODUCTION

The research objective of this paper is to establish a baseline study on the differences in Convective Heat Transfer Coefficient (CHTC) between a bare roof and a roof with photovoltaic panels (PVs). This will give an idea on whether the differences are relevant and whether further research and more refined numerical modelling is viable.

Knowledge of the CCHTC on building surfaces has been studied extensively in the past years (for example: Sharples [1], Hagishima & Tanimoto [2]). This is because this quantity has a fundamental role in the assessment of building energy performance. Most types of whole-building simulation tools make use of standard formulae or in some cases constant values of CHTC for the entire building envelope. Mirsadeghi *et al.* [3] give a detailed review of how these models are adopted into building energy simulation programs.

Studies which specifically target roof surfaces are much less common due to the complex flow field resulting at this location. An empirical correlation applicable to horizontal roofs has also been developed by Clear *et al.* [4] which conclude that the CHTC follows closely the correlation for flat plates in turbulent boundary layers but has to be scaled by a factor of around 1.6. An experimental analysis was carried out by Shao *et al.* [5], which was compared with other models such as that by Emmel *et al.* [6], Cole *et al.* [7] and also Clear *et al.* [4]. Their results highlight large differences between predictions. The authors attribute this difference to the variable conditions assumed such as surface roughness, turbulence levels, building geometries, *etc.* Other experimental work on CHTCs, including that on roofs has been discussed by Defraeye *et al.* [8] but the authors emphasize that the CFD comparisons for roofs show large differences when different turbulence models are used. The authors suggest the use of unsteady turbulence formulations such as URANS (Unsteady Reynolds Averaged Navier Stokes) or Large Eddy Simulation (LES).

The analysis of the influence of Photovoltaic (PV) panels on roofs has been given attention in previous studies. The emphasis is however mostly on the shading effect against direct sun irradiation on roofs (examples include Dominguez *et al.* [9], Tian *et al.* [10], Yang [11] and Ouyang *et al.* [12]). There has also been a numerical study by Jubayer [13] and Karava *et al.* [14] on building integrated photovoltaics on sloped roofs. In these studies the authors make use of both steady and transient approaches. Another study which is more relevant

to the present work is the Stereo Particle Image Velocimetry investigation of the flow on roof having PVs at different angles RANS (refer to Pratt *et al.* [15]). The authors describe in detail the resulting flow physics involved in such a scenario.

The issue of the effect of PVs on the CHTC is as yet not fully explored; mainly due to the complexity of the flow prevalent on roof tops.

2 METHODOLOGY

A numerical methodology is adopted in this research by solving the Navier Stokes and energy equations using the commercial code ANSYS Fluent® 15.0 [16]. This approach enables full-field information to be obtained which is essential for a preliminary analysis of the problem. The COST CFD guideline document under COST Action 732 [17] and the AIJ guideline paper by Tominaga *et al.* [18] are used as a reference for guiding the CFD analysis of an isolated building. This ensures that the method follows established standards given the lack of experimental measurements.

2.1 Fluid flow and heat transfer models

The continuity equation (conservation of mass) for an incompressible flow is given as follows:

$$\frac{\partial u}{\partial x}+\frac{\partial v}{\partial y}+\frac{\partial w}{\partial z}=0 \qquad (1)$$

Where x, y and z are the Cartesian coordinates and u, v, w are the velocities in the *x*, *y* and *z* directions.

The momentum equations in vector form are given by:

$$\rho\vec{v}\cdot\vec{\nabla}\vec{v}=-\vec{\nabla}p+\mu\vec{\nabla}^2\vec{v}+\vec{F} \qquad (2)$$

Where $\vec{v}$ is the velocity vector, ρ is the density, p is the pressure, μ is the dynamic viscosity and $\vec{F}$ is the body force vector.

The energy equation is given by:

$$\rho c_p\left(\frac{\partial Tu}{\partial x}+\frac{\partial Tv}{\partial y}+\frac{\partial Tw}{\partial z}\right)=\frac{\partial}{\partial x}\left(k\frac{\partial T}{\partial x}+u\tau\right)+\frac{\partial}{\partial y}\left(k\frac{\partial T}{\partial y}+v\tau\right)+\frac{\partial}{\partial z}\left(k\frac{\partial T}{\partial z}+w\tau\right) \qquad (3)$$

Where *T* is the temperature, *k* is the thermal conductivity of air and τ is the viscous shear stress.

For a more complete description of these equations the reader is referred to text books such as Versteeg [19].

2.2 Problem description

An isolated 10m by 10m by 10m building block is considered for this analysis. This case study is similar to the one investigated by Defraeye *et al.* [8]. The ground and building temperature is assumed to be constant at 40°C during a typical hot summer day in Malta. The atmospheric temperature is set at 30°C. The PV panels are assumed to be isothermal bodies with a temperature of 70°C as found in Mavromatakis *et al.* [20]. The described scenario is shown in Figure 1. The configuration and dimensions of the PV panels are shown in **Figure 2**. These dimensions are kept fixed throughout all simulations.

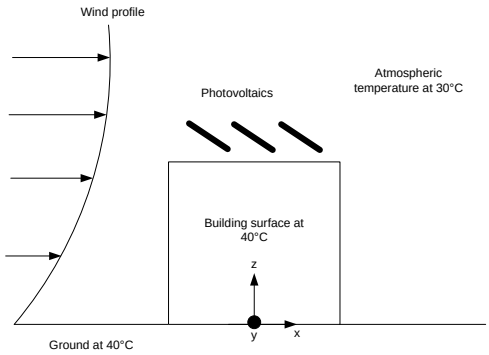

Figure 1: Problem schematic.

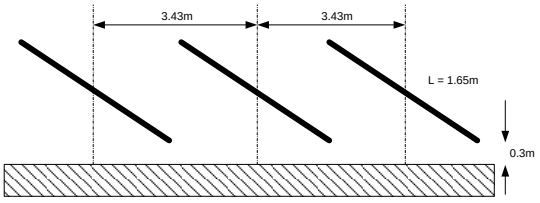

Figure 2: PV panel geometry and configuration.

2.3 Model description

The domain has dimensions of 21H length along the North wind direction, 11H along the width and 6H in height, where H is the building height (10m). These ensure that the boundaries of the model do not interfere with the flow on the building. The blockage ratio is assumed at 1.5%.

In order to appropriately capture the thermal gradients on walls, wall functions cannot be used to approximate the shape of this boundary layer. For this reason, a Low Reynold's Number Modelling (LRNM) approach is used as indicated by Defraeye *et al.* [17]. Inherently, LRNM cannot account for surface roughness. Also, the y+ value in near wall regions needs to be around 1, where:

$$y^+=\frac{\sqrt{\tau_w/\rho}\,y_p}{\upsilon} \qquad (4)$$

Where τ_w is the wall shear stress, υ is the air kinematic viscosity and y_p is the distance from the wall and the first adjacent cell centre.

A tetrahedral mesh is used around the building with substantial wall refinement to capture the velocity gradients in the sub-layer. The distance from the wall to the centre of the first adjacent cell is taken as 0.01μm to ensure that y+ values are 1 or smaller. For the rest of the domain, a mapped mesh is used. Figure 3 shows the mesh structure close to the panels and far away from the building.

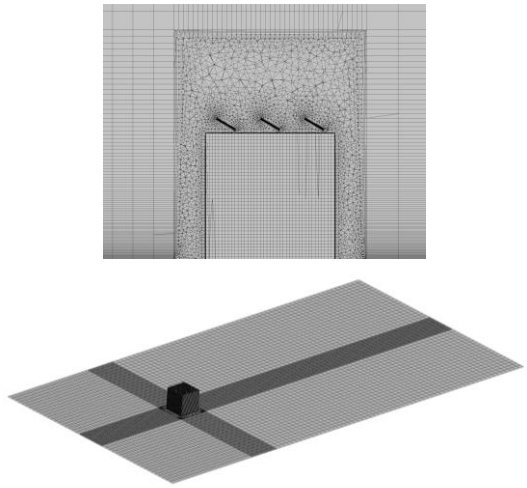

Figure 3: Mesh used for the CFD model.

The Richardson number was found to be around 0.2 which is much less than unity and hence only forced convection heat transfer is considered (natural convection effects ignored).

The parameters of air which were used are given in Table 1.

Table 1 - Properties of air used in the simulations.

Density [kg/m3]	1.225
Dynamic viscosity [kg/ms]	1.79e-5
Conductivity [W/mK]	0.0242
Specific heat capacity [kJ/kgK]	1.006

2.4 Wind and Turbulence modelling

The inlet is prescribed as a velocity profile which follows the following logarithmic law:

$$U = \frac{u*}{\kappa}\ln\left(\frac{z+z_0}{z_0}\right) \quad (5)$$

Where $u*$ is the atmospheric boundary layer friction velocity, κ = 0.4187 is the von Karman constant, z is the height above ground level and z_0 is the aerodynamic roughness length. This is taken to be the same as used by Defraeye *et al.* [8] as 0.03m. The wind inlet wind speed at building height is assumed as 4m/s for all tests carried out in this study.

The turbulent kinetic energy (TKE) profile of the velocity inlet is taken as:

$$k = 3.3u*^2 \quad (6)$$

The turbulent dissipation rate profile of the velocity inlet is on the other hand:

$$\varepsilon = \frac{u*^3}{\kappa(z+z_0)} \quad (7)$$

Both of the quantities are taken as given in Defraeye *et al.* [8]. As a general note, the wind profile should remain constant as it progresses from inlet up to the building region. Due to the fact that surface roughness cannot be modelled, stream-wise gradients in the wind flow will result which is unavoidable.

3 RESULTS

3.1 Flow characteristics on roofs with and without PVs

Before analysing the CHTC on the roofs, it is important to first consider the flow physics on the roof. Fundamental studies on isolated buildings using CFD started more or less in the late seventies including works from Blocken *et al.* [21]. In this study, a steady RANS approach is used. This has various limitations particularly in the overestimation of turbulent kinetic energy at the windward roof corner which results in a small recirculation zone. Figure 4 shows the velocity magnitude resulting from a roof with no PV and a roof with a PV under North and North-Westerly winds. For the north wind case, the slow wind speed indicates the recirculation region which extends up to more than half of the length. For the north-westerly wind the view only shows a smaller reduction in speed. With the PVs included, the flow exhibits a substantial slowdown due to the separation from the wind-ward PV panels. The downwind PV panels interact with the wake of the upstream panel. Some acceleration of the flow can be observed at roof level on the upstream row of PV panels. For the north-west wind scenario, the resulting flow shows less slow-down downstream of the PV panels as a result of the different aerodynamic loading on the panels. These flow characteristics have an important bearing on the resulting CHTC values.

The turbulent kinetic energy (TKE) is plotted in Figure 5. This quantity is also of particular importance to the predicted CHTC values. For the North wind case with no PV, the large TKE at the roof windward corner is clearly visible. With more advanced modelling such as Large Eddy Simulation, this is expected to be lower.

For the case with PVs, the TKE is small in the downwind panel row regions but remains high above the PV panels. For the north-westerly wind case, the TKE reduces overall, both with as well as without PVs.

As stated, the limitations with the current k-ε model will have an affect on the prediction capability of this model. Nonetheless, for a preliminary investigation, the results obtained for the CHTC should be indicative of what happens under the influence of the PV panels.

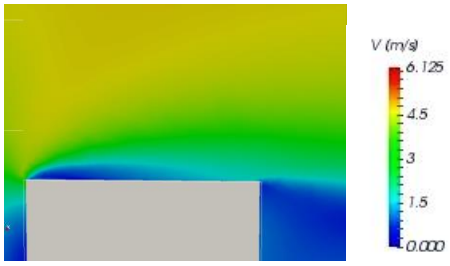

(a) North wind, no PVs

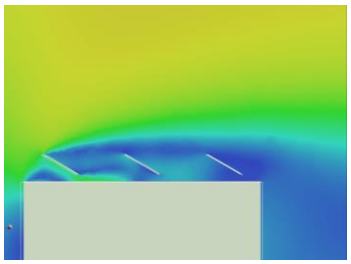

(b) North wind, with PVs

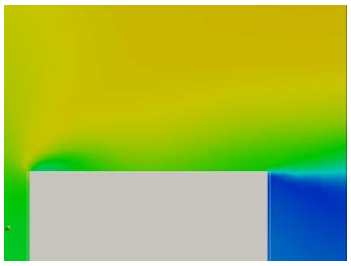

(c) North-west wind, no PVs

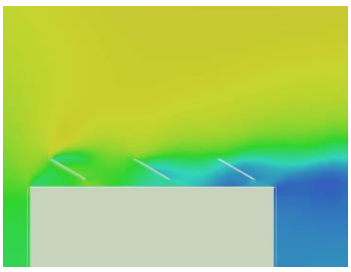

(d) North-west wind, with PVs

Figure 4: Velocity magnitude in a side plane view for various configurations. The free-stream flow in the x-direction is directed from left to right.

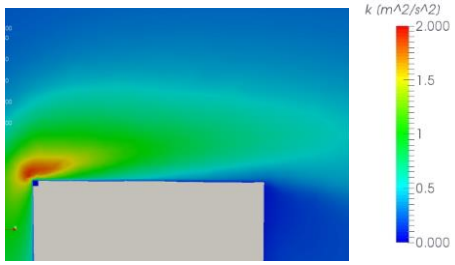

(a) North wind, no PVs

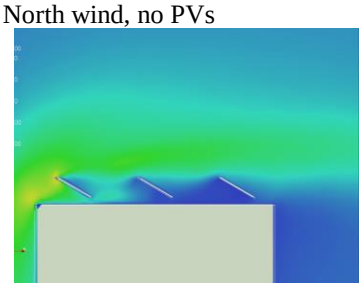

(b) North wind, with PVs

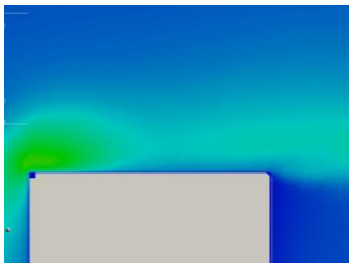

(c) North-west wind, no PVs

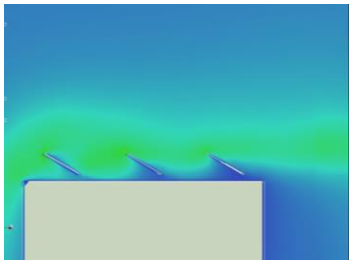

(d) North wind, PVs

Figure 5: Turbulent kinetic energy (TKE) for various configurations in a side plane view. The free-stream flow in the x-direction is directed from left to right.

3.2 Roof thermal boundary layer

The thermal boundary layer results for all tested conditions are given in Figure 6. The value of the CHTC is dependent on the gradient of this temperature profile over the roof surface. The temperature difference between the building surface and the atmosphere is 10°C. Three locations are plotted which correspond to the centre of each row of PV panels. The gradient close to the building surface varies only slightly for the case of no PVs. This result is further emphasized for the North-westerly wind case with no PVs.

For the case with PVs, there are substantial differences between the temperature profile gradients. Particularly, the upwind PV panel position shows a much higher thermal gradient compared to the downstream PV panels. Also clear is the temperature reached by the bulk fluid well above the roof surface. Due to the temperature of 70°C imposed on the PV panels, the air is heated in the presence of the upstream panels. This increase in temperature is around 6°C and does not show any further increase at the downstream PV panel.

For the north-westerly wind cases, there are also some differences in the gradients at each PV panel position. The bulk temperature of the fluid (away from the roof surface) varies between all PV panel positions. The differences are however less than the case of the north wind as a result of the smaller wind velocity in the *x*-direction.

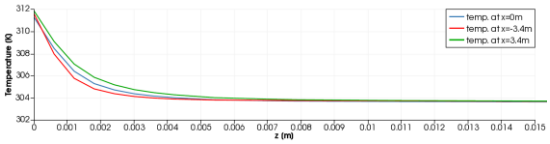

(a) North wind, no PV

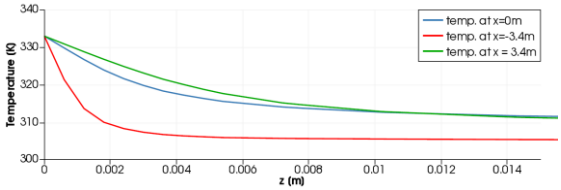

(b) North wind, no PV

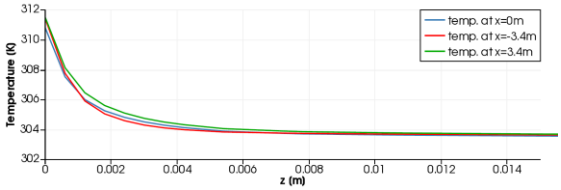

(c) North-west wind, no PVs

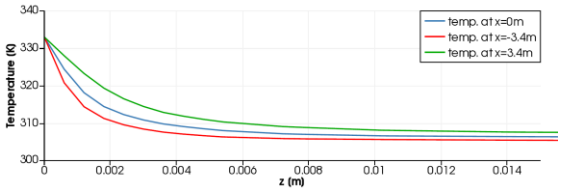

(d) North-westerly wind with PVs

Figure 6: Boundary layer temperature profile at the PV locations *x*=0, *x*=-3.4m and *x*=3.4m.

3.3 Roof CHTCs with and without PVs

The results for the CHTC on the roof surfaces are shown in Figure 7. The variations in the CHTC values across the bare roof are rather small compared to the case with PVs. A slightly higher CHTC can be observed on the windward edge of the roof in the north wind case. This is qualitatively consistent with the findings by Defraeye *et al.* [8].

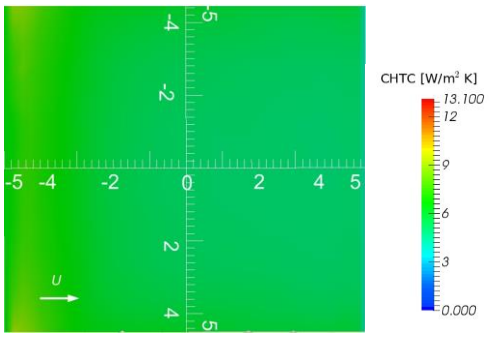

(a) North wind, no PVs

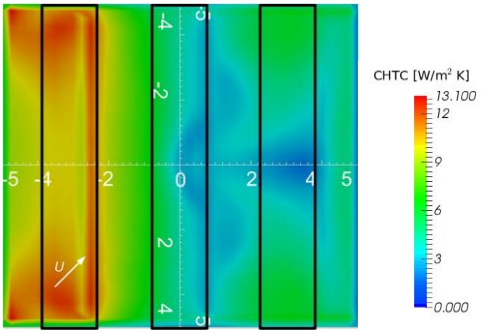

(b) North wind, with PVs

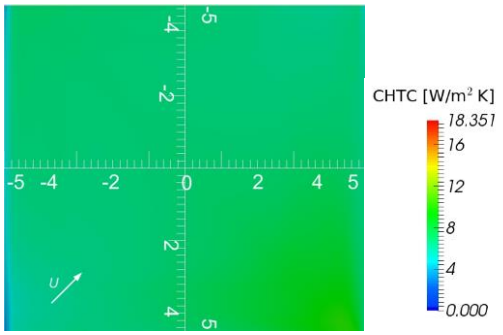

(c) North-west wind, no PVs

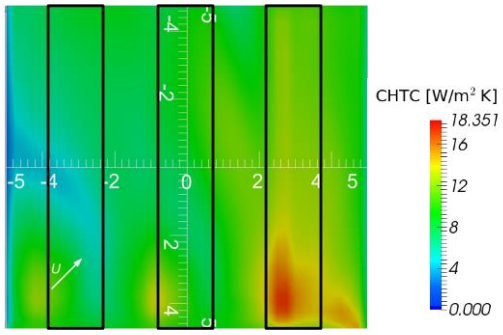

(d) North-west wind, with PVs

Figure 7: Roof CHTC for various configurations.

For the rest of the roof the variability is minimal. In the presence of PVs, substantial variations can be observed, which are consistent with what is observed for the thermal boundary layer profiles of Figure 6. In the region of the upwind row of panels, there is substantial increase

in the CHTC, reaching levels of around 13W/m^{2}K. For the downwind panel regions, the opposite happens; there is a substantial reduction in CHTC. This trend is a direct implication of the variation of the TKE since increased TKE will result in an increase in the CHTC.

For a north-westerly wind, the variability in CHTC is also minimal across the entire roof as is the case with the north wind situation. There are some decreases and increases on the north and west sides of the roof as a result of the recirculation regions in these locations. For the situation with PVs present, the variation in CHTC over the roof is rather complex. A small CHTC is apparent on the north side of the roof. At the panel locations, there is an increase in CHTC near the west edge of the roof. This effect increases from row to row moving downstream where the last row experiences the largest CHTC. This effect is due to the added turbulence intensity due to the wake of the upwind rows.

These results are summarised in Table 2 along with the analytical solution result of the average CHTC in the case of a flow over a flat plate in a turbulent boundary layer (refer to Incropera *et al.* [22]). The results are all smaller than the analytical solution as a result of the fundamentally different flow conditions present for a cube immersed in the atmospheric boundary layer.

Table 2: CHTC (in W/m^{2}K) for all configurations tested. The analytical solution is based on a flat plate turbulent boundary layer result.

	No PV	**PV**
N (CFD)	5.72	7.19
NW (CFD)	6.69	9.28
Analytical	9.85	

4 DISCUSSION

The applicability of this research cannot be seen in isolation but rather as an element for the basis of calculating the overall heat transfer coefficient, or U-Value of a typical roofing element.

Considering a typical roof made up of a 150mm reinforced concrete (having a thermal conductivity (λ) of 2.5 W/mK), externally topped with a layer of 100mm *Torba* (λ - 0.8W/mK), a 75mm screed layer (λ – 1.93W/mK) and a 4mm light finished roofing felt (λ – 0.23W/mK) and internally finished with a 4mm ceiling plasterboard (λ – 0.21W/mK), the total U-Value for the building element assuming the calculated convective heat transfer coefficients is as shown in Table 3. The indoor heat transfer coefficient is assumed to be 7.2W/m^{2}K)

Table 3: Calculated U-Value (W/m^{2}K) for all configurations tested.

	N	**NW**
No PV	1.74	1.82
PV	1.85	1.97

The difference in U-Value for the two calculated values is in the range of 6.6% (North facing) and 8.2% (North-West facing). Considering that this is an involuntary bi-product of installing a conventional photovoltaic system on a roof, such a result cannot be neglected, especially in summer when the photovoltaic panels will shade the roof thus decreasing solar gains and potentially, as shown by the results aid in removing heat from inside the building.

Adding insulation, on the other hand practically nullifies this difference as in this case the insulation is the predominant component, making up the U-value of the building element.

5 CONCLUSIONS

This preliminary numerical study has shown that for typical summer temperature conditions, the presence of PV panels has a tendency to increase the magnitude of the CHTC due to the increased turbulence generated by the panels. This is expected but this paper quantifies these differences albeit with a rather simplified approach. The effect on the percentage increase in U-values using typical Maltese roof constructions has shown that, at least for the summer season, the roof is more ventilated. The percentage increase in U-value was shown to increase for North-westerly winds which are more predominant in the Maltese climate.

It is acknowledged that experimental validation of these results would be necessary. Moreover, the numerical model shall be improved in near future research to:

1. Make use of a more suitable turbulence model such as either URANS or LES as suggested by Defraeye *et al.* [17].
2. To perform a sensitivity analysis on the numerical results.

More work is also needed on the relationship between the average Nusselt number on the roof and the *Re* number since in this study, only a single *Re* number is considered.

6 SCOPE FOR FURTHER RESEARCH

Beyond this study, there are other options not considered here. These deepen the study and open up the scope for further research:

- ❖ Computational modelling is but one aspect of thermal modelling and simulation. Another equally important approach would be to model a selected number of building forms in an urban context through a scale model in a wind tunnel. Here various angles for the PV array could be tested, also simulating these in tandem with the wind tunnel modelling.
- ❖ This study was principally concerned with the flat roof being a smooth surface. Hence the results achieved are based on this prerogative. Therefore another aspect not considered here would be the surface roughness of the flat roof. This is particularly important since in Malta, apart from smooth concrete screed (power float finish), one may have a textured roof membrane or a synthetic turf surface.
- ❖ Other alternative options could include changing the height of the parapet wall or including a higher structure on one side of the PV array, as is typically the case with a stairwell, lift machine room or other services.

7 REFERENCES

[1] S. Sharples, «Full-scale measurements of wind-induced convective heat transfer from a roof-mounted flat plate solar collector,» *Build. Environ.*, pp. 31-39, 1984.

[2] A. Hagishima e J. Tanimoto, «Field measurements for estimating the convective heat transfer coefficient at building surfaces,» *Building and Environment*, vol. 38, pp. 873-881, 2003.

[3] M. Mirsadeghi, D. Costola, B. Blocken e J. Hensen, «Review of external convective heat transfer coefficient models in building energy simulation programs: implementation and uncertainty,» *Applied Thermal Engineering*, vol. 56, n. 1-2, pp. 134-151, 2013.

[4] R. Clear, L. Gartland e F. Winkelman, «An empirical correlation for the outside convective air-film coefficient for horizontal roofs.,» *Energy and Buildings*, vol. 35, n. 8, pp. 797-811, 2003.

[5] J. Shao, J. Liu, J. Zhao, W. Zhang, D. Sun e Z. Fu, «A novel method for full-scale measurement of the external convective heat transfer coefficient for building horizontal roof,» *Energy and Buildings*, vol. 41, n. 8, pp. 840-847, 2009.

[6] M. Emmel, M. Abadie e N. Mendes, «New external convective heat transfer coefficient correlations for isolated low-rise buildings,» *Energy and Buildings*, vol. 39, pp. 335-342, 2007.

[7] R. Cole e N. Sturrock, «The convective heat exchange at the external surface of buildings,» *Building and Environment*, vol. 12, pp. 207-214, 1977.

[8] T. Defraeye, B. Blocken e J. Carmeliet, «Convective heat transfer coefficients for exterior building surfaces: Existing correlations and CFD modelling,» *Energy Conversion and Management*, vol. 52, n. 1, pp. 512-522, 2011.

[9] A. Dominguez, J. Kleissl e J. Luvall, «Effects of solar photovoltaic panels on roof heat transfer,» *Solar Energy*, vol. 85, n. 9, pp. 2244-2255, 2011.

[10] W. Tian, Y. Wang, Y. Xie, D. Wu, L. Zhu e J. Ren, «Effect of building integrated photovoltaics on microclimate of urban canopy layer,» *Building and Environment*, vol. 42, pp. 1891-1901, 2007.

[11] H. Yang, H. Burnett, Z. Zhu e L. Lu, «A simulation study on the energy performance of photovoltaic roofs,» *ASHRAE Transactions*, vol. 107, n. 2, pp. 129-135, 2001.

[12] W. S. Ouyang, P. Khai Ng e Jie'er, «Study of the partial shading impact on the PV roof in zero energy building in Singapore with PVSYST simulation,» in *IBPSA*, Sydney, 2011.

[13] C. M. Jubayer, P. Karava e E. Savory, «Building-Integrated Photovoltaic/Thermal Systems – Numerical Prediction of Exterior Convective Heat Transfer Coefficients and Parametric Analysis,» in *Internation High Performance Building Conference*, Purdue University, 2010.

[14] P. Karava, C. M. Jubayer e E. and Savory, «Numerical modelling of forced convective heat transfer from the inclined windward roof of an isolated low-rise building with application to photovoltaic/thermal systems,» *Applied Thermal Engineering*, vol. 31, pp. 1950-1963, 2011.

[15] R. N. Pratt e R. N. Kopp, «Velocity measurements around low-profile, tilted, solar arrays mounted on large flat-roofs, for wall normal wind directions,» *Journal of Wind Engineering and Industrial Aerodynamics*, vol. 123, pp. 226-238, 2013.

[16] ANSYS - Simulation Driven Product Development. Fluent version 15.0. 2014.

[17] COST Action 732 - Quality Assurance and improvement of microscale meteoreogical models, «Best Practice Guideline for the CFD simulation of flows in the urban environment,» COST office, Brussels, 2007.

[18] Y. Tominaga, Y. Mochida, R. Yoshie, H. Kataoka, T. Nozu, M. Yoshikawa e T. Shirasawa, «AIJ guidelines for practical applications of CFD to pedestrian wind environment around buildings,» *Journal of Wind Engineering and Industrial Aerodynamics*, vol. 96, pp. 1749-1761, 2008.

[19] H. Versteeg e W. Malalasekera, An introduction to Computational Fluid Dynamics The Finite Volume Method, London: Pearson: Prentice Hall, 2007.

[20] F. Mavromatakis, E. Kavoussanaki, F. Vignola e Y. Franghiadakis, «Measuring and estimating the temperature of photovoltaic modules,» *Solar Energy*, vol. 110, pp. 656-666, 2014.

[21] B. Blocken, T. Stathopoulos, J. Carmeliet e L. Jan, «Application of computational fluid dynamics in building performance simulation for the outdoor environment: an overview,» *Journal of Building*

Performance Simulation, vol. 4, n. 2, 2011.

[22] Incropera, Dewitt, Bergman e Lavine, Fundamentals of Heat and Mass Transfer, Wiley, 2006.